Correlations in quantum dots

Wolfgang Häusler

Correlations in quantum dots

Wolfgang Häusler

I. Institut für Theoretische Physik, Universität Hamburg, Jungiusstrasse 9, D-20355 Hamburg, Germany

Abstract. The lowest excitations of a repulsively interacting few particle system are investigated within correlated "pocket state" basis functions. For long range interaction and non–isotropic confining potentials the method becomes exact, in the limit of large mean inter–particle distances r_s. The multiplet structure of the many–electron energy levels is explained and the ratios δ between the lowest excitation energies, which are related to the electron spin, are determined quantitatively using group theoretical means. The δ are independent of the detailed form of the inter–particle repulsion and of sufficiently large r_s. The obtained δ–values are confirmed by available numerical data. The method is applied to 1D and 2D quantum dots.

1. Introduction

Advanced nanostructuring techniques on the basis of high mobility semiconductor hetero–structures allow to isolate finite numbers of electrons from the 2D bulk material by means of suitably shaped gate electrodes or by etching techniques [1]. These *quantum dots* [1–5], contain sometimes less than $N = 10$ electrons [6].

Quantum dots show the single electron phenomena [7] like the Coulomb blockade [8], the single electron tunneling oscillations [9] and the periodic conductance oscillations [3] due to the high value of the energy $e^2/2C$ associated with the addition or removal of one single electron of charge e. For systems containing only few electrons [6, 10], a proper definition of a (charge independent) capacitance C is difficult [11, 12]. This reflects the importance of correlations due to the Coulomb interaction on top of the charging energy in absence of an effective screening mechanism in semiconductor systems at low electron densities.

For a 1D model has been shown numerically and explained in terms of localized charge density distributions [11] that for mean electron distances r_s larger than the Bohr radius $a_B = \varepsilon \hbar^2/me^2$ (which depends on the material through the dielectric constant ε and the effective mass m) non of the lowest excitation energies scale like $\sim L^{-2}$ with the typical diameter L of the system. The level spectrum is considerably modified by interactions. It has been demonstrated that the Hartree Fock approach is not reliable to describe ground state properties in 1D [13] and in 2D [14].

Bosonization techniques can be applied to 1D systems of infinite size if the dispersion of the non–interacting part of the Hamiltonian is linear. This means that scattering events are assumed to take place only in the vicinity of the two Fermi points. Various correlation functions have been determined [15] but only very recently indications of a crystallization of the (charge) density–density correlation function have been found in presence of long range Coulomb interactions [16]. However, the almost vanishing density–density correlation function at short distances [17] has not been reproduced and is possibly not contained in the linearized model. For calculations of conductance properties [18, 19] the existence of a Wigner crystal is frequently presumed [20]. Spin involving excitations are usually ignored within this class of models.

The correlation effects in quantum dots influence qualitatively spectral [11, 14, 21, 22, 23] and transport [24, 12] properties. Non–linear transport involves excited states [4, 5, 25, 26, 27] of the correlated electrons [28]. To determine the many–electron excitations in a confined system by using its symmetry is the main purpose of the present work. Without further spatial symmetries the permutations S_N of N elements constitute the only unalienable symmetry for N identical particles. In the particular case of an isotropic harmonic potential in 2D the group theoretical classification has been given recently [29]. A group theoretical analysis should be applied to a suitably chosen N-particle basis rather than to (effective) one-electron states.

After specifying the particular model in Sect. 2 the lowest excitation energies of a finite number of repulsively interacting particles confined in a quantum dot will be determined in Sect. 3. To satisfying approximation the low lying spectrum can be expressed in terms of only *one* parameter that, being a tunneling integral, varies exponentially with r_s. The accuracy of the description presented here is increasing with increasing relative influence of the interaction compared to the kinetic energy when $r_s \gg a_B$, correlation effects are fully taken into account. The ratios between the lowest excitation energies are shown to be insensitive to the detailed form of the repulsive interaction between the particles, they depend only on N and the shape (which includes the dimensionality) of the quantum dot. In Sect. 4 the physically realized many Fermion or Boson states will be selected using group theory. The resulting spectra for one- and two-dimensional models of quantum dots are presented in Sects. 5 and 6. They are compared with available numerical data. Final conclusions are drawn in Sect. 7.

2. Model

An N-particle quantum dot without magnetic field is described by the Hamiltonian

$$H = \sum_{i=1}^{N} \left(\frac{p_i^2}{2m} + v(x_i) \right) + W(x_1, \ldots, x_N)$$

$$W(x_1, \ldots, x_N) = \frac{1}{2} \sum_{\substack{i,j \\ i \neq j}} w(|x_i - x_j|), \tag{1}$$

x_i and p_i are position and momentum of the i'th particle in d dimensions with (effective) mass m and spin s. The dot confinement $v(x)$ and the interaction $w(x)$ both do not depend on spin. The 2D-case $v(x) \sim x^2$, $w(|x|) \sim 1/|x|$ has been investigated for $N = 2$ [21] and $N = 3$ [23] electrons.

A 1D square well

$$v(x) = V_0 \Theta(|x| - L/2), \quad V_0 \gg \pi^2 N^2 / mL^2$$

$$w(x) = e^2 \frac{e^{-\alpha|x|}}{\varepsilon \sqrt{x^2 + \lambda^2}}, \quad \lambda \ll L \tag{2}$$

has been studied for $N \leq 4$ [22, 11, 17] and (2) will be the specific example in Sect. 3. A (small) transversal spread of the wave functions is described by λ and α^{-1} is the range of the interaction.

At large mean inter-particle distance $r_s \equiv L/(N - 1) \gtrsim 100\, a_B$ the charge density distribution in the ground state is inhomogeneous and, for $\alpha = 0$, shows N well separated peaks. This behaviour is due to the dominant Coulomb energy compared to the kinetic energy, and is known as "Wigner crystallization". In absence of a true phase transition in 1D and 2D, it reflects the short distance behaviour of the density–density correlation function. The charge density between the peaks in the investigated finite system is almost vanishing [17]. The quantum mechanical ground state energy at large r_s is much better

approximated by equidistantly located classical point charges than by a homogeneous charge distribution [11]. Like in 3D [30] the excitations in the low density limit can be described as phonon like vibrations of the charges around their equilibrium positions due to (linearized) Coulomb forces between them. These excitations scale $\sim r_s^{-\gamma}$ with the particle density, γ is close [11] to 3/2 [30]. In the limit $r_s \gtrsim 100\, a_B$ the spectrum is independent of the statistics of the particles, Fermionic or Bosonic, cf. Sect. 5.

For electrons with $s = 1/2$ the vibrational levels are 2^N-fold spin–degenerate. When r_s decreases to intermediate values $a_B < r_s < 100\, a_B$ these levels start to split exponentially [11] into a finite number of sub-levels. The following part of the paper is devoted to describe this resulting *fine structure* of lowest excitation energies in few electron quantum dot systems.

3. Pocket states

For Hamiltonians not explicitly depending on spin like (2) the eigenenergies are solely determined from spatial space (they correspond to solutions of a differential equation with boundary conditions). Ignoring in the following the identity and the spin of the particles increases the Hilbert space (for the not necessarily (anti-) symmetric functions) and leads to an increased number of resulting eigenvalues. Later in Sect. 4.2 the Fermionic or Bosonic space will be restored and the extra eigenvalues will drop out. For N distinguishable particles the Hamiltonian (1) can be conceived as describing *one* particle in a space of $N \cdot d$ dimensions.

3.1. Single particle description

If $d = 1$, as in (2), the configuration space is a (hyper-) cube L^N where the repulsive interaction W establishes potential barriers (at least of height e^2/λ). W separates the minima of the total potential $\sum_i v(x_i) + W$. In absence of symmetries, as in 1D, there are $N!$ minima which for like particles are equivalent, i.e. they transform into one another by permuting their coordinates. In 2D the number of minima can be a multiple of $N!$, this case will be discussed in Sect. 6. The minima are located on a hyper–ring in configuration space (i.e. a $(N - 2)$-dimensional manifold) perpendicular to the main diagonal of the (hyper–) cube L^N. The center of the ring coincides with the center of the cube. Every minimum is surrounded by $N - 1$ nearest neighbouring minima at equal distances.

3.2. Pocket state approximation (PSA)

To solve the one particle quantum mechanics at low energies I use an approximation familiar from the treatment of the symmetric double well with a potential $V(x) = V(-x)$ as sketched in Fig. 1 for a one-dimensional configuration space. The Hilbert space is restricted to two "pocket" states $|L\rangle$ and $|R\rangle$ each peaked around one minimum of V. Time reversal symmetry is not broken,
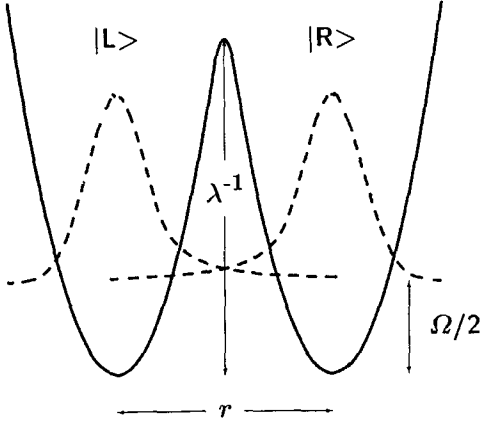
Fig. 1. Double minimum potential, schematically. If $\langle L|H|R\rangle \ll \Omega$ the Hilbert space can be restricted to span$\{|L\rangle, |R\rangle\}$ to describe the lowest excitation.

therefore $0 \leq \langle x|L\rangle = \langle -x|R\rangle$ and both states are related to one another by the mirror symmetry. The ground state is approximated as the symmetric, the first excited state as the antisymmetric linear combination of both basis functions. The energy difference Δ between the corresponding eigenvalues is proportional to the matrix element $\langle L|H|R\rangle$ of the Hamiltonian that describes tunneling between left and right. This approximation is good if the barrier between both potential minima is high so that

$$\Delta \ll \Omega. \tag{3}$$

Ω is the energy of higher excitations in the double well. To describe higher excited states nodes have to be introduced which cannot be approximated by $|L\rangle$ and $|R\rangle$.

Due to the exponential decay of $\langle x|L\rangle$ and $\langle x|R\rangle$ under the barrier Δ decreases exponentially with increasing distance r between the minima and $\Delta \sim \exp(-\lambda^{-1/2})$ with increasing height λ^{-1} of the barrier. If Ω decreases only algebraically with r (3) is fulfilled at sufficiently large r justifying then the truncation of the Hilbert space to span$\{|L\rangle, |R\rangle\}$.

The problem discussed in Sect. 3.1 can be treated in similar spirit. The pocket state approximation (PSA) is not limited to one–dimensional or translationally invariant (tight binding) potentials [31]. The Hilbert space is truncated to span$\{|p\rangle\}$ of $1 \leq p \leq N!$ states, in coordinate representation $\langle x_1, \ldots, x_N|p\rangle$ each being strongly peaked around one certain potential minimum and small elsewhere. The elements of the Hamiltonian matrix H

$$H_{pp'} \equiv \langle p|H|p'\rangle$$

describe *correlated* tunneling between two different *arrangements* p and p' of the N particles. The basis $\{|p\rangle\}$ accounts for correlations. The ground state has the same symmetry as the Hamiltonian and is given by the linear combination

$$\frac{1}{\sqrt{N!}} \sum_{p=1}^{N!} |p\rangle. \tag{4}$$

The inhomogeneous charge density

$$\rho(x) = \frac{1}{(N-1)!} \sum_{p,p'} \int dx_2 \ldots dx_N \langle x, x_2, \ldots, x_N|p\rangle$$

$$\langle p'|x, x_2, \ldots, x_N\rangle, \tag{5}$$

obtained in [17], reflects the separation of different probability amplitudes $\langle x_1, \ldots, x_N|p\rangle$ and $\langle x_1, \ldots, x_N|p'\rangle$.

The one to one correspondence between pocket states $|p\rangle$ and permutations $p \in S_N$ is established through the multiplication

$$p'' = p \cdot p' \Leftrightarrow \langle x_1, \ldots, x_N|p''\rangle = \langle x_{p(1)}, \ldots, x_{p(N)}|p'\rangle$$

where $p(i)$ is the permutation of the sequence $i = 1, \ldots, N$. All pocket states are similar in shape due to the equivalence of the potential minima. The $\{|p\rangle\}$ form a regular representation of S_N, and therefore standard group theoretical arguments, cf. [32], can be applied. Each irreducible representation (IR) Γ occurs d_Γ-times in a regular representation where d_Γ is the dimensionality of Γ (cf. Sect. 4.2).

In the symmetrized basis

$$P_\Gamma \text{ span}\{|p\rangle\} \tag{6}$$

the Hamiltonian matrix becomes block diagonal. The projectors

$$P_\Gamma := \sum_{p \in S_N} \chi^\Gamma(p) \mathcal{C}(p) \tag{7}$$

are determined by the (real) characters $\chi^\Gamma(p)$ of IR Γ to the element $p \in S_N$ (cf. Sect. 4.2). Up to S_7 the $\chi^\Gamma(p)$ are tabulated e.g. in [32]. $\mathcal{C}(p)$ performs the permutation p on the vector space span$\{|p\rangle\}$.

In the following some general properties of the Hamiltonian matrix in the basis $\{|p\rangle\}$ will be proven. It is convenient to consider the traceless matrix M

$$M_{pp'} := H_{pp'} - H_{pp}\delta_{pp'}. \tag{8}$$

Since H_{pp} does not depend on p, H and M differ only by a unit matrix and are both block diagonal in the basis (6). If only entries $M_{pp'}$ are significantly different from zero where p and p' differ by *odd* permutations (like single transpositions, this is the case for the dominant off-diagonal $H_{pp'}$ studied in the present work, cf. Sect. 3.3), each eigenvalue ε of M associated with a Γ-symmetric eigenvector has a counterpart $-\varepsilon$ corresponding to an eigenvector of adjoined symmetry $\bar\Gamma$ (cf. Sect. 4.1). This follows from the property $\chi^\Gamma(p) = \pm \chi^\Gamma(p)$, depending on the parity (± 1) of p. Thus the spectrum of M is symmetrically distributed around $\varepsilon = 0$. If the eigenvalue ε is associated with a Fermion state $-\varepsilon$ represents a Bose state, see Sect. 5, so that in particular for the 1D model (2) the highest Fermion eigenvalue is spin polarized.

The rapid decay of $\langle x_1, \ldots, x_N|p\rangle$ with distance allows furthermore to neglect all $H_{pp'}$ with p' being not one of the $N-1$ nearest neighbours of p in L^N. Then the $M_{pp'}$ may approximatively be either zero or equal to one common constant t_N (the rows and the columns of M still represent S_N) which causes all eigenvalues of M to be proportional to t_N. In Sect. 3.3 is shown that this assumption is to good approximation valid.

The $H_{pp'} \sim \exp(-\sqrt{r_s/r_c})$ scale roughly exponentially with r_s if $r_s > r_c$ (cf. the following Section). On the other hand the separation between different level multiplets $\Omega \sim r_s^{-\gamma}$ decrease only algebraically which justifies the PSA according to (3) at sufficiently large r_s (Sect. 5). The density scale r_c^{-1} is determined by (3) and separates the regimes of weak and strong interaction. It characterizes the applicability of PSA.

The vibrational excitations of typical energies Ω can be conceived as the discrete energy level spectrum of the particle introduced in Sect. 3.1 being confined in one particular potential pocket. The applicability of the PSA can in principle be extended to higher excited states by including more than one pocket state per site so that nodal (hyper-) planes can be incorporated. The lowest of the vibrational excitations is related to the collective motion of all particles in phase (acoustic mode). It is parallel to the main diagonal of the cube L^N and thus perpendicular to the (hyper-) plane where all potential minima are located (cf. Sect. 3.1). No additional p'- dependence is introduced to the non-vanishing overlap integrals $H_{pp'}$ and the ratios (cf. Sect. 3.3) between the splittings within the lowest and within the first excited vibrational level multiplets should be equal. This is no longer true for higher vibrational excitations when nodal planes parallel to the main diagonal of L^N are introduced. Then the sequence of fine structure levels changes quantitatively though each multiplet still contains the same frequency of total spin S states (cf. Sect. 4.2) and the same total amount of states.

The lowest vibrational excitation energy decreases with increasing N at constant r_s. This is why the pocket state description is restricted to systems of finite sizes. In the thermodynamic limit the acoustic mode evolves into the zero energy Goldstone mode so that (3) is violated and the low energy spectrum is no longer determined by well separated multiplets with 'universal' internal structure.

3.3. WKB Approximation

To compare the magnitudes of the most important off–diagonal entries $H_{pp'}$ for the 1D example (2) a semi-classical method is used. This approach can be generalized correspondingly to different situations like higher dimensionalities. The locations $x^{(p)} \equiv (x_1^{(p)}, \ldots, x_N^{(p)})$ of adjacent potential minima in L^N differ just in one transposition of two coordinates $x_i^{(p)}$ and $x_j^{(p)}$ with $|x_i^{(p)} - x_j^{(p)}| = \sqrt{2}\,r_s$. Accordingly, the dominant $H_{pp'}$ corresponds to an interchange of adjacent electrons in the N-electron chain (2). In the following will be shown that the value of the corresponding overlap integral does not depend very much on the position k ($1 \leq k \leq N - 1$) along the chain where the exchange takes place. The k-dependence of $H_{pp'}$ can be estimated within (simplified) WKB approximation. Only regarding the exponentially varying part [33] yields

$$H_{pp'} \sim \exp - \int_0^{\mathcal{T}} d\tau \left(\frac{m}{2}(\dot{x}(\tau))^2 + W(x(\tau)) \right). \tag{9}$$

The path $x(\tau)$ connects p at $\tau = 0$ with p' at $\tau = \mathcal{T}$ and minimizes the action (9) connected with the motion in the negative potential $-W(x(\tau))$. $\mathcal{T}$ is the period for that motion.

The problem to find the extremal path will be simplified by taking just the straight line for $x(\tau)$ connecting p with p'. This disregards the motion of other electrons apart from the two considered ones during the time $\mathcal{T}$ and can be justified for small values of λ in (2) when the height of the potential saddle is dominated by λ^{-1} and slight variations in the positions of the other electrons modify this value only little. In 2D situations (1) this "adiabatic" simplification is in general not valid.

The (imaginary) time integration in (9) then becomes

$$H_{pp'} \sim \exp - \sqrt{2}\, r_s \int_0^1 dq \sqrt{2m(W(x(q)) - W(x(0)))} \tag{10}$$

by virtue of energy conservation $-\frac{m}{2}(\dot{x}(\tau))^2 + W(x(\tau)) = W(x(0)) = W(x(\mathcal{T}))$ along $x(\tau)$. The factor $\sqrt{2}$ accounts for the two masses carried from p to p'. For the interaction $w(x) = \frac{e^2}{\varepsilon}(x^2 + \lambda^2)^{-1/2}$ in (2)

$$H_{pp'} \sim \exp\left[-A_{N;k} \sqrt{\frac{L}{a_B} \frac{2\varepsilon}{N-1}} \right] \tag{11}$$

where

$$A_{N;k} \equiv \int_0^1 dq \left[\tilde{w}(2q-1) - \tilde{w}(1) \right.$$

$$+ \frac{1}{2} \sum_{\substack{i=1 \\ i \neq k, k+1}}^{N} \{ \tilde{w}(k-i+q) - \tilde{w}(k-i)$$

$$\left. + \tilde{w}(k+1-i-q) - \tilde{w}(k+1-i) \} \right],$$

$$\tilde{w}(q) \equiv (q^2 + \ell^2)^{-1/2}, \quad \ell \equiv \lambda/r_s = (N-1)\lambda/L$$

contains the k-dependence of the WKB-action associated with interchange of adjacent electrons in the chain. $A_{N;k}$ still depends weakly on N and λ.

The numerical data shown in Fig. 5 of [11] at low densities agree with a $\log(\Delta) \sim -\sqrt{L}$ behaviour. The N-dependence obtained in [11] is however less pronounced than suggested by (11). This indicates a pronounced dependence of the prefactor on the dimensionality N of the configuration space which has been ignored in (9). In Fig. 2 $A_{N;k}$ is plotted for various N and $\lambda/L = 2 \cdot 10^{-4}$ as used in [11]. The variation of $A_{N;k}$, less than 2% of their mean value, leads to significant k-dependencies of $H_{pp'}$ only if $r_s \gtrsim 35\, a_B$. But then the magnitude of $H_{pp'}$ has decreased already to unobservable small values so that the fine structure splitting disappears and the system consists of classical electrons (Wigner molecule). Increasing λ/L to values up to 0.1 reduces the mean value of $A_{N;k}$ but leaves their relative variations with k almost unaffected. If the interaction is modified by an additional cutoff ($\alpha > 0$ in (2)) the k-dependence of $A_{N;k}$ becomes even weaker. For given electron number this justifies to assume all non-vanishing $H_{pp'} \equiv t_N$ to be equal in 1D. According to Sect. 3.2 equal non-vanishing off-diagonal elements of
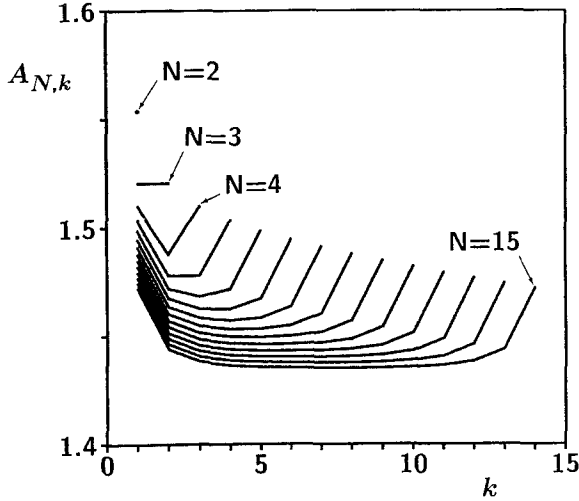
Fig. 2. $A_{N;k}$ as defined in the text versus the position k along the chain for $\lambda/L = 2.10^{-4}$ and various N. The exchange of two adjacent particles close to the boundary leads to a slightly smaller overlap integral than other non-vanishing $H_{pp'}$. These variations with k can be neglected compared to the mean value of $A_{N,k}$

$H_{pp'}$ yield differences between the eigenvalues being proportional to t_N and thus to ratios being independent of the parameters like r_s, λ or α (cf. (2)). These ratios are not affected by the detailed shape of the inter-particle repulsion $w(x)$. Only a non-zero range is required for $w(x)$ to cause the exponentially small overlap between adjacent pocket states.

4. Symmetries

Appropriate use of symmetry facilitates understanding and computation of eigenstates and transition rates [32]. Since the Hamiltonian commutes with the elements of a symmetry group, its eigenfunctions transform according to the irreducible representations (IR) Γ of this group. The Hilbert space $\mathcal{H}$ of wave functions can be decomposed into orthogonal subspaces $\mathcal{H}_\Gamma$

$$\mathcal{H} = \bigoplus_\Gamma \mathcal{H}_\Gamma \tag{12}$$

so that the Hamiltonian matrix in a symmetrized basis is block diagonal. This can considerably simplify a numerical diagonalization. Mostly the property (12) is employed to single particle states, as obtained e.g. within molecular field approximation. In the following (12) is applied to the pocket state basis to select the appropriate eigenvalues from the spectrum obtained in Sect. 3 that satisfy the Pauli principle for identical Fermions or Bosons carrying spin.

The indistinguishability of like particles requires that any eigenfunction of (1)

$$\psi(x_1\sigma_1, \ldots, x_N\sigma_N)$$

belongs to the one-dimensional (anti)symmetric IR of S_N with respect to permutations among the *enumeration* of

the particles. These permutations affect position x_j and spin σ_j of the jth particle simultaneously.

Apart from this unalienable symmetry, in absence of spin-orbit coupling, the Hamiltonian (1) is also invariant under *separate* permutations of the $\{\hat{x}_1, \ldots, \hat{x}_N\}$ and $\{\hat{\sigma}_1, \ldots, \hat{\sigma}_N\}$ operators. Therefore ψ transforms additionally according to IR Γ_x and Γ_σ of the group of permutations among the spatial and the spin degrees, respectively. Both permutation groups are isomorphous to S_N.

4.1. The symmetry group S_N

A few properties of the symmetric group (cf. [32]) should be summarized here. All irreducible representations (IR) Γ of S_N can be labeled uniquely by the partitions

$$[n_1, \ldots, n_N] \tag{13}$$

of ordered sequences of positive integers obeying

$$n_i \geq 0, \sum_{i=1}^N n_i = N, \quad n_i \geq n_{i+1} \text{ for } 1 \leq i \leq N.$$

E.g. $[1, \ldots, 1]$ and $[N]$ denote the antisymmetric and the symmetric IR respectively ($n_i = 0$ is not written).

The only factor group of S_N is isomorphous to S_2 implying the existence of an adjoined IR $\bar{\Gamma}$ to every Γ of equal dimensionality and equal moduli for the characters $|\chi^\Gamma(p)| = |\chi^{\bar{\Gamma}}(p)|$. From the orthogonality relations among characters follows that Kronecker products

$$\Gamma_1 \times \Gamma_2 \text{ contain } \begin{Bmatrix} [1, \ldots, 1] \\ [N] \end{Bmatrix} \quad \text{only if } \begin{cases} \Gamma_1 = \bar{\Gamma}_2 \\ \Gamma_1 = \Gamma_2 \end{cases}. \tag{14}$$

4.2. Physically realized many particle states

Though ψ is in general no product of a spatial and a spin function, the Pauli principle requires that the Kronecker product

$$\Gamma_x \times \Gamma_\sigma \times \begin{Bmatrix} [1, \ldots, 1] \\ [N] \end{Bmatrix} \neq \varnothing \quad \text{for } \begin{cases} \text{Fermions} \\ \text{Bosons} \end{cases}$$

must contain the (anti)symmetric IR. Thus with (14)

$$\begin{Bmatrix} \Gamma_\sigma = \bar{\Gamma}_x \\ \Gamma_\sigma = \Gamma_x \end{Bmatrix} \quad \text{for } \begin{cases} \text{Fermions} \\ \text{Bosons} \end{cases}. \tag{15}$$

For example spinless particles (i.e. $\Gamma_\sigma = [N]$) must transform according to $[1, \ldots, 1]$ or $[N]$ in spatial space.

Also for particles with spin $s = 1/2$ ψ cannot transform according to any IR of S_N under permutations of $\{\sigma_1, \ldots, \sigma_N\}$. Only the IR's $\Gamma_\sigma = [n_1, n_2]$ occur [34], where $n_1 = N/2 + S$ and $n_2 = N/2 - S$ are related to the total spin S. For electrons

$$\Gamma_\sigma = [N/2 + S, N/2 - S] \tag{16}$$

means that S fixes Γ_σ and therefore Γ_x (15). S can take integer or half integer values.

States with aligned spins $S = N/2$ are associated with an antisymmetric spatial state $\Gamma_x = [1, \ldots, 1]$. Γ_x can only be equal to $[N]$ if $\Gamma_\sigma = [N/2, N/2] = [1, 1]$ is antisymmetric, i.e. for $N = 2$. Only in case of two electrons the (symmetric) ground state of $H_{pp'}$ can be realized (cf. Sect. 5).

The dimensionalities $d_{[n_1, n_2]}$ of the IR's (16) can be expressed explicitly [34]

$$d_{[N/2+S, N/2-S]} = \frac{(2S + 1)N!}{(N/2 + S + 1)!(N/2 - S)!} \quad (17)$$

in terms of N and S. They are equal to the frequency of appearances of a given IR $\Gamma = [N/2 + S, N/2 - S]$ in a regular representation. Thus

$$d_{[N/2+S, N/2-S]} \leq \kappa_{N,S} \quad (18)$$

gives a lower bound to the number $\kappa_{N,S}$ of eigenvalues of the Hamilton matrix in the pocket state basis to a given total spin S. In absence of further symmetries in spatial space, like in 1D, (18) becomes an equality. Because of the $(2S + 1)$-fold Zeeman degeneracy of each fine structure level the sum

$$\sum_{S=0 \text{ or } 1/2}^{N/2} (2S + 1)d_{[N/2+S, N/2-S]} = 2^N$$

is equal to the dimensionality of the spin space.

The cases $s > 1/2$ will not be discussed here. For Fermions and Bosons the generalization is in principle straightforward though the number of possible Γ_σ increases and the unique relation to S (16) is lost.

5. Results for the 1D model (2)

For low electron numbers the individual blocks of the Hamiltonian matrix in the symmetrized basis (6) can be diagonalized analytically, in 1D up to $N \leq 4$. The results are given in Table 1 in units of t_N. Fine structure spectra for $N = 5$ and $N = 6$, shown in Figure 4, are obtained by

Table 1. Analytical values for the fine structure spectrum $E_\nu^{(N)}$ of model (2) within PSA for $N \leq 4$. S is the total spin of N Fermions with $s = 1/2$. The excitation energies $E_\nu^{(N)} - E_{\text{Bose}}^{(N)}$, in units of t_N, refer to the eigenvalue $E_{\text{Bose}}^{(N)}$ of the symmetric linear combination of pocket states (4) which is the lowest eigenvalue and corresponds to the $s = 0$ Bosonic ground state

N	S	$E_\nu^{(N)} - E_{\text{Bose}}^{(N)}$
2	0	0
2	1	$2t_2$
3	1/2	t_3
3	1/2	$3t_3$
3	3/2	$4t_3$
4	0	$(3 - \sqrt{3})t_4$
4	1	$(4 - \sqrt{2})t_4$
4	1	$4t_4$
4	0	$(3 + \sqrt{3})t_4$
4	1	$(4 + \sqrt{2})t_4$
4	2	$6t_4$

Fig. 3. Ratio $\delta \equiv \Delta_2/\Delta_1$ between two fine structure energy differences for $N = 3$ versus r_s as indicated in the inset. Within PSA $\delta = 1/2$, cf. Table 1. Below $r_s \gtrsim 0.3\, a_B$ the third excited state is of spin $S = 1/2$ which makes the definition of δ ambiguous

Fig. 4. Fine structure multiplets for $N = 3, \ldots, 6$ as obtained within PSA (pock). The numerical values (dashed) are obtained as in [11] (num) for systems of length $L = 11.3\, a_B, N = 3$ and $L = 13.2\, a_B, N = 4$. The N-dependence of t_N is not considered, t_N has been adjusted to normalize the overall width of the multiplets

numerical diagonalization of blocks of sizes 25×25 and 81×81, respectively. The diagonalization of the full Hamiltonian in the basis of non–interacting electrons, as carried out in [11], was possible only for $N \leq 4$ including a sufficient number of single particle levels to get accurately the fine structure. These data are included in Figure 4. The sizes of the matrices were typically 15000×15000. Not only the sequence of spin values is described correctly within PSA but also the quantitative ratios δ among the distances between the levels.

Lieb and Mattis [35] have proven that for a finite electron system in 1D

$$E(S) > E(S') \text{ if } S > S'. \quad (19)$$

$E(S)$ is the lowest energy eigenvalue of the system to given spin S. Nothing is required for the interaction $w(x)$ between the electrons but boundedness and independence of spin. Consequently the ground state is either $S = 0$ or $S = 1/2$. All fine structure spectra shown in Fig. 4 obey (19).

The state with polarized spins $S = N/2$ is, according to (15), totally symmetric $\Gamma_x = [N]$ in spatial space for (fictitious) Bosons with spins $s = 1/2$ and therefore the ground state (4) of the matrix M defined in (8). From the properties of the eigenvalues of M described in Sect. 3.2 and from $[\bar{N}] = [1, \ldots, 1]$ follows for $s = 1/2$ Fermions that *the spin polarized state $S = N/2$ is the energetically highest state within the lowest vibrational multiplet*. This state occurs according to (17) and (18) only once because $d_{[N]} = 1$. The argument can even be generalized to two dimensional quantum dots if there is only $v = 1$ classical electron configuration of lowest energy, cf. Sect. 6.2 and 7. According to [28] the $S = N/2$ state plays a particular role for the transport through a quantum dot at finite applied voltages – it leads to negative differential conductances. This state would be the Fermion ground state if spin was ignored. Insofar the interacting electron system lowers its ground state energy using the spin degree of freedom. This has been found recently also for the 3D Wigner crystal [36].

The approach of the numerically obtained ratios between excitation energies to the values obtained within the pocket state description with increasing r_s determines again a scale r_c of electron distances separating the almost non-interacting regime from the regime of strong correlations so that for $r_s > r_c$ the PSA becomes valid. In Fig. 3 the ratios between the two lowest excitation energies are shown for $N = 3$. The value $r_c \approx 1.7\,a_B$ estimated assuming an exponential approach agrees nicely with the value extracted from the decay of Δ_1 [11] and from the onset of the charge density distribution to show N peaks [17].

6. Results for 2D quantum dots

Well separated peaks appear in the one particle distribution at low densities also in finite systems of higher dimensionalities if continuous symmetries are absent. Then the lowest spin involving excitations can be described using pocket states. Like in 1D the spectrum shows vibrational levels that split due to tunneling between different electron arrangements. The important difference to 1D are the reduced heights of the potential barriers, the electrons can interchange their positions more easily by surrounding each other. Some of the connecting paths involve just slight changes of electron distances, so that the tails of the long range Coulomb interaction creates only shallow barriers between the locations of the potential minima. Then the PSA fails if $w(x)$ is only short range. Furthermore, the PSA requires electron densities r_c^{-2} smaller than in 1D to provide small kinetic energies and sufficient separations of the electron arrangements. Nevertheless, the scaling behaviours $\Delta \sim \exp(-\sqrt{r_s/r_c})$ of spin sensitive and $\Omega \sim r_s^{-\gamma}$ of vibrational excitations are still different, and $\Delta \ll \Omega$ is established for sufficiently large r_s.

The two dimensional case is particularly relevant to hetero-structures. Numerical results for excitation spectra of Coulombically interacting electrons in rectangular, hard wall quantum dots [12] at low electron densities are available only for $N = 2$ [37]. Figures 1 and 2 of [37] confirm the expected grouping of the levels with increasing system size L into vibrational multiplets with internal

structure. A considerably larger value for r_c compared to $1.7\,a_B$ can be estimated from these figures.

6.1. Quasi 1D case

The striking similarities between vibrational and fine structure excitations of two electrons in a 2D hard wall rectangle of length L and width $L/10$ (Fig. 1 in [37]) and the corresponding spectrum for a 1D square well box (Fig. 1 in [11]) can be understood by the large width u of the pocket state wave function. In the narrow rectangular system [37] u would be estimated by linearizing the interaction $e^2/\varepsilon(x - r_s)$ for $x \ll r_s$

$$\frac{u}{a_B} \approx \frac{1}{2}\left(\frac{21}{4}\pi\right)^{2/3}\left(\frac{r_s}{a_B}\right)^{2/3}$$

to be larger $u \gtrsim L/10$ than the width of the rectangle as long as $r_s = L < 3 \times 10^4 a_B$. Then transversal excitation energies $\sim \pi^2(10/L)^2$ exceed longitudinal vibrational or fine structure excitations. The system is quasi one-dimensional and its spectrum can be approximated by putting $\lambda/L = 0.1$ in (2).

6.2. Square shaped dots

To understand the spectrum for a hard wall square, Fig. 2 of [37], within PSA the method described in Sect. 3 has to be generalized. The substitutional single particle (Sect. 3.1) moves now in the configuration space L^{2N}. The number of potential minima may be a multiple v of $N!$ if there exist v energetically equivalent classical electron configurations for the repulsively interacting electrons. This is the case e.g. already for $N = 2$ where $v = 2$.

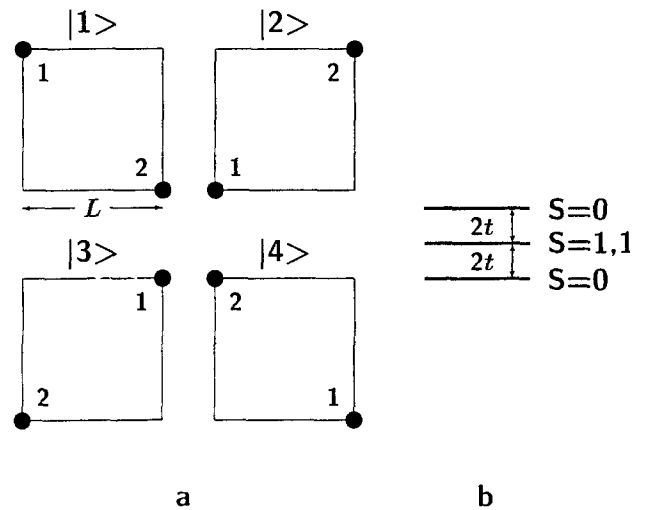The 4 pocket states describing two electrons in a square for large r_s are illustrated in Fig. 5a. The

Fig. 5 **a.** The 4 equivalent arrangements of minimal inter-particle repulsion for $N = 2$ electrons on a square that form the 4 pocket states. **b** The resulting fine structure spectrum consists of 3 levels at equal distances and total spins S as indicated

dominant overlap integrals between them are of type $\langle 1|H|2\rangle = \langle 1|H|3\rangle$. Due to the longer tunneling path overlap integrals like $\langle 1|H|4\rangle$, which corresponds to the permutation of two like particles, are much smaller. Neglecting the latter and classifying the obtained eigenstates according to their transformation properties with respect to *permutations among the particle enumeration* leads to a fine structure spectrum as shown in Fig. 5b. The multiplet contains in total $v \cdot 2^N$ states (including Zeeman degeneracies). The ground state is a symmetric linear combination of these 4 pocket states. The one particle density (5) shows 4 peaks of equal weight in the 4 corners, each containing a charge $e/2$. In any dimensions the ground state of two interacting electrons has minimal spin $S = 0$ (cf. [35]). Removal of the square symmetry (cf. Sect. 7) would cause the two degenerate $S = 1$ states to split.

Three electrons in the classical ground state configuration are again preferably located in the corners of the square in $v = 4$ possible ways so that tunneling into the empty place is the dominant process. The fine structure nmultiplet is determined by $4 \cdot 3! = 24$ pocket states. Considering only the dominant overlap integral yields a spectrum shown in Figure 6. There are in total $4 \cdot 2^3 = 32$ states in the multiplet.

Four and five electrons in a square have only $v = 1$ classical ground state configuration. The number of pocket states is 4! and 5! respectively. For $N = 5$ the dominant tunneling process is the exchange of the central electron with one of the electrons sitting on the corners. The corresponding path is of shortest length and involves only 2 electron masses. For $N = 4$ it is not so obvious which if the two possible paths for transitions between different permutations of the electrons sitting one at each corner prevails: *i)* the rotation of all four electron positions simultaneously by 90° (ring exchange) *ii)* the exchange of just two adjacent electrons leaving the remaining two unaffected. In one case the mass and in the other case the height of the potential barrier is larger. Assuming straight lines like in (10) for the paths in configuration space L^{2N} the action corresponding to *i)* can be expressed as a single integral with the numerical value $1.6\hbar\sqrt{\varepsilon L/a_B}$. In the second case even the spatial trajectory is difficult to determine, how the two electrons surround each other. A rough estimate for the action connected with this latter exchange may be obtained by the following linear path during the time $\mathcal{T}$: the first electron moves along one edge of the square, passing half the way at time $\mathcal{T}/2$ while the second electron moves along two pieces of straight lines, bending halfway at the position of the lowest saddle point of the potential. The numerical value of the action connected with this latter path is $1.1\hbar\sqrt{\varepsilon L/a_B}$. Both imaginary time actions are upper limits to the true classical values and the approximation *ii)* is surely worse compared to *i)*. Therefore the pair exchange of adjacent electrons should be the slightly favourable process. Neglecting all other processes leads to a fine structure spectrum for four electrons as it is shown in Fig. 6. However, the difference between the two paths is not very pronounced so that entries due to the ring exchange into the Hamiltonian matrix can modify the $N = 4$ fine structure if $r_s = L$ is not very large.
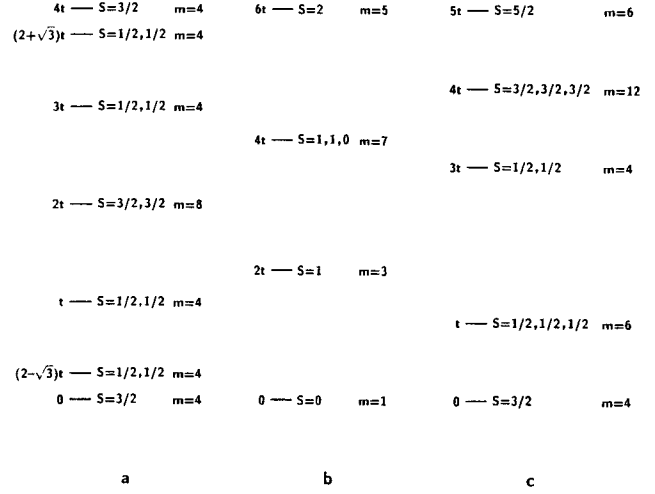

Fig. 6. Fine structure spectra of a $N = 3$, b $N = 4$, c $N = 5$ electrons in a 2D square within PSA in units of t. The spin values S and the number of states m per level are indicated. The tunneling integrals t are described in the text

A prominent property of the obtained correlated eigenstates in 2D are values of ground state spins, which, in contrast to 1D, are not the lowest possible ones. The three electron ground state becomes spin polarized and also has the five electron ground state spin $S = 3/2$ in the square shaped quantum dot at low electron densities. This proves the inapplicability of the Lieb and Mattis Theorem to higher dimensionalities if $N > 2$. The ground state spin values influence crucially both the linear and the non–linear transport behaviour of 2D quantum dots [39].

Cases with larger electron numbers can in principle be treated analogously if $\Delta \ll \Omega$ is fulfilled. With increasing N this requires a decreasing electron density because:

1. the vibrational energies $\Omega \sim 2\pi e/(N - 1)^{1/d} \sqrt{\varepsilon m r_s^3}$ decrease with increasing size of the system due to acoustic modes
2. the barriers between equivalent electron arrangements decrease so that Δ increases (cf. [17]).

The first point depends only on the electron density while the second point makes the pocket state approximation less reliable in say three dimensional situations.

7. Summary and conclusions

Excitation spectra of repulsively interacting, highly correlated few electron systems have been investigated in 1D and 2D. This is particularly important for semiconductor based single electron experiments using quantum dots, where electron correlations can dominate over the kinetic energy so that the energy spectra differ qualitatively [12] from the non–interacting situation. The lowest levels bunch up to multiplets and neither inter– nor intra–multiplet energy differences scale like $\sim L^{-2}$ with the system diameter [11]. The spectrum is explained in terms of correlated many–particle "pocket states". The inter–multiplet distances, corresponding to vibrational excitations

due to Coulomb forces between localized electrons [17] are independent of Fermion or Boson statistics. The fine structure splitting of each multiplet is caused by correlated motions connecting different arrangements of the particles and reveals Fermionic or Bosonic statistics and spin. The number of levels to a certain total spin S within each multiplet is given by (17) for any number of electrons. The splitting is proportional to tunneling integrals between different pocket sites.

At sufficiently large r_s only one of the tunneling integrals dominates exponentially. Then the ratios δ between the fine structure energies are independent of the detailed form of the repulsion between the particles and of r_s. Quantitative spectra for the 1D quantum dot with hard walls are shown in Table 1 and Fig. 4 up to $N \leq 6$. The comparison with numerically obtained ratios δ yields the scale $r_c \approx 1.7\ a_B$, found also in [11, 17], that separates weak from strong interaction regime. "Slim" quantum dots should behave effectively one–dimensional if they are narrower than the pocket state.

Depending on the shape of a 2D quantum dot, discrete symmetries of the confining potential can lead to $v > 1$ possible arrangements already of classical electrons to equally minimal electrostatic energy. The total number of eigenvalues in a multiplet, including Zeeman degeneracy, is then $v \cdot 2^N$. Symmetries which led to $v > 1$, however, are likely to be removed in polarizable environments for the following reason. The energetically most favourable places for the quantum dot electrons depend on the distribution of surrounding (non-conducting) charges which themselves are influenced by the distribution of the (conducting) dot charges. In this way the dot electrons can adjust their environment to lower the total energy. For example, two electrons in a square will easily polarize their surrounding, leaving rather a diamond shaped configuration for the potential. The interplay between the surrounding and the granular electron density of the dot finally tends to reduce the number of equivalent minima in configuration space to its minimal value $N!$, the number of permutations of N particles. Classical ground state energies being unequal only on the scale of the tunneling integral t_N suffices. The shape of the quantum dot depends additionally on voltages applied to side gates [3] so that the fine structure spectra can change with gate voltage.

The lowest eigenstates in 2D can be approximated within the pocket state basis if the inter-particle repulsion decays slower than $\sim |x|^{-2}$. Then many of the qualitative results obtained for the few electron quantum dot in 1D are valid in 2D. This concerns in particular the exponential dependence of the excitation energies and the independence of the ratios between them on r_s. If $v = 1$ the spin polarized state is of highest energy within the lowest vibrational multiplet. As example a square shaped quantum dot has been investigated. Larger ground state spin polarizations are found than $S = 0$ or $S = 1/2$ of non–interacting or 1D electrons. The Lieb and Mattis–theorem is inapplicable to systems of higher dimensionality if $N > 2$.

It would be interesting to measure the total spins of the ground states, perhaps by sophisticated ESR-experiments [38]. They influence the linear and the non–linear conductance [39]. The electron states of aligned spins

$S = N/2$ play a distinguished role for non-linear transport properties of quantum dots. They can cause negative differential conductances [28]. Furthermore, the observed dependencies on a magnetic field [27] oriented along the current [40] can be explained in a natural way by the Zeeman splitting of the many-electron states [41].

References

1. Kastner, M.A.: Rev. Mod. Phys. **64**,849 (1992)
2. Sikorski, Ch., Merkt, U.: Phys. Rev. Lett. **62**, 2164 (1989)
3. Meirav, U., Kastner, M.A., Wind, S.J.: Phys. Rev. Lett. **65**, 771 (1990); Kouwenhoven, L.P., van der Vaart, N.C., Johnson, A.T., Kool, W., Harmanns, C.J.P.M., Williamson, J.G., Staring, A.A.M., Foxon, C.T.: Z. Phys. B **85**, 367 (1991); Heinzel, T., Manus, S., Wharam, D.A., Kotthaus, J.P., Böhm, G., Klein, W., Tränkle, G., Weimann, G.: Europhys. Lett. **26**, 689 (1994)
4. Johnson, A.T., Kouwenhoven, L.P., de Jong W., van der Vaart, N.C., Harmanns, C.J.P.M., Foxon, C.T.: Phys. Rev. Lett. **69**, 1592 (1992)
5. Weis, J., Haug, R.J., v. Klitzing, K., Ploog, K.: Phys. Rev. B **46**, 12837 (1992)
6. Meurer, B., Heitmann, D., Ploog, K.: Phys. Rev. Lett. **68**. 1371 (1992); Ashoori, R.C., Stormer, H.L., Weiner, J.S., Pfeiffer, L.N., Pearton, S.J., Baldwin, K.W., West, K.W.: Phys. Rev. Lett. **68**, 3088 (1992); Ashoori, R.C., Stormer, H.L., Weiner, J.S., Pfeiffer, L.N., Baldwin, K.W., West, K. W.: Phys. Rev. Lett. **71**, 613 (1993)
7. Averin, D.V., Likharev, K. K.: J. Low Temp. Phys. **62**, 345 (1986); A good review can be found in: Grabert, H., Devoret, M., (eds.) Single Charge Tunneling NATO ASI Series vol. 294. New York: Plenum Press 1992
8. Devoret, M.H., Esteve, D., Grabert, H., Ingold, G.-L., Pothier, H., Urbina, C.: Phys. Rev. Lett. **64**, 1824 (1990)
9. Delsing, P., Likharev, K.K., Kuzmin, L.S., Claeson, T.: Phys. Rev. Lett. **63**, 1861 (1989)
10. Sikorski, Ch., Merkt, U.: Surf. Sci. **229**, 282 (1990)
11. Häusler, W., Kramer, B.: Phys. Rev. B **47**, 16353 (1993)
12. Palacios J. J., Martin-Moreno L., Tejedor C.: Europhys. Lett. **23**, 495 (1993); Palacios, J.J.: PhD thesis, Universidad Autónoma de Madrid. (1993)
13. Mašek, J.: (unpublished)
14. Hawrylak, P., Pfannkuche, D.: Phys. Rev. Lett. **70**, 485 (1993)
15. Sólyom, J.: Adv. Phys. **28**, 201 (1979); Mahan, G. D.: Many–Particle Physics. New York, London: Plenum Press 1990
16. Schulz, H. J.: Phys. Rev. Lett. **71**, 1864 (1993)
17. Jauregui, K., Häusler, W., Kramer, B.: Europhys. Lett. **24**, 581 (1993)
18. Apel. W.: J. Phys.: Condens. Matter **16**, 2907 (1983)
19. Kane, C.L., Fisher M. P.A.: Phys. Rev. Lett. **68**. 1220 (1992)
20. Glazman, L.I., Ruzin, I.M., Shklovskii, B.I.: Phys. Rev. B **45**, 8454 (1992); Averin D.V., Nazarov Yu. V.: Phys. Rev. B **47**, 9944 (1993)
21. Merkt, U., Huser, J., Wagner, M.: Phys. Rev. B **43**, 7320 (1991); Pfannkuche, D., Gerhards, R. R.: Phys. Rev. B **44**, 13132 (1991)
22. Häusler, W., Kramer, B., Mašek, J.: Z. Phys. B **85**, 435 (1991)
23. Pfannkuche, D., Gudmundsson, V., Maksym P.A.: Phys. Rev. B **47**, 2244 (1993)

560

24. Meir, Y., Wingreen, N.S., Lee, P.A.: Phys. Rev. Lett. **66**, 3048 (1991); Kinaret, J.M., Meir, Y., Wingreen, N.S., Lee, P.A., Wen, X.G.: Phys. Rev. B **46**, 4681 (1992)
25. Averin, D.V., Korotkov, A.N., Likharev, K.K.: Phys. Rev. B **44**, 6199 (1991)
26. Foxman, E.B., McEuen, P.L., Meirav, U., Wingreen, N.S., Meir, Y., Belk, P.A., Belk, N.R., Kastner, M.A., Wind, S.J.: Phys. Rev. B **47**, 10020 (1993); Bruder, C., Schoeller, H.: Phys. Rev. Lett. **72**, 1076 (1994)
27. Nicholls, J.T., Frost, J.E.F., Pepper, M., Ritchie, D.A., Grimshaw, M.P., Jones, G. A.: Phys. Rev. B **48**, 8866 (1993)
28. Weinmann, D., Häusler, W., Pfaff, W., Kramer, B., Weiss, U.: Europhys. Lett. **26**, 689 (1994)
29. Haase, R.W., Johnson, N.F.: Phys. Rev. B **48**, 1583 (1993)
30. Meissner, G., Namaizawa, H., Voss, M.: Phys. Rev. B **13**, 1370 (1976)
31. Hüller, A., Kroll, D.M.: J. Chem. Phys. **63**, 4495 (1975)
32. Hamermesh, M.: Group Theory and its Applications to Physical Problems new edition. New York: Dover 1989
33. Schulman, L.S.: Techniques and Applications of Path Integration: New York: John Wiley & Sons 1981
34. Inui, T., Tanabe, Y., Onodera, Y.: Solid State Sciences. Berlin: Springer 1990
35. Lieb, E., Mattis, D.: Phys. Rev. **125**, 164 (1962)
36. Moulopoulos, K., Ashcroft, N. W.: Phys. Rev. Lett. **69**, 2555 (1992)
37. Bryant, G.W.: Phys. Rev. Lett. **59**, 1140 (1987)
38. Ghosh, R.N., Silsbee, R.H.: Phys. Rev. B **46**, 12508 (1992)
39. Weinmann, D., Häusler, W., Kramer, B.: Phys. Rev. Lett. **74**, 984 (1995)
40. Weis, J., Haug, R.J., v. Klitzing, K., Ploog, K.: Phys. Rev. Lett. **71**, 4019 (1993)
41. Pfaff, W., Weinmann, D., Häusler, W., Kramer, B., Weiss, U.: Z. Phys. B **96**, 201 (1994)